Available online at www.sciencedirect.com
SCIENCE DIRECT
Ocean Modelling 12 (2006) 416–435
Ocean Modelling
www.elsevier.com/locate/ocemod

Sensitivity of a global ocean model to increased run-off from Greenland

Rüdiger Gerdes [a,*], William Hurlin [b], Stephen M. Griffies [b]

[a] *Alfred-Wegener-Institut für Polar- und Meeresforschung, Bussestr. 24, 27570 Bremerhaven, Germany*
[b] *NOAA Geophysical Fluid Dynamics Laboratory, Princeton University Forrestal Campus, 201 Forrestal Road, Princeton, NJ 08540-6649, USA*

Received 22 June 2005; received in revised form 9 August 2005; accepted 30 August 2005
Available online 17 October 2005

Abstract

We study the reaction of a global ocean–sea ice model to an increase of fresh water input into the northern North Atlantic under different surface boundary conditions, ranging from simple restoring of surface salinity to the use of an energy balance model (EBM) for the atmosphere. The anomalous fresh water flux is distributed around Greenland, reflecting increased melting of the Greenland ice sheet and increasing fresh water export from the Arctic Ocean. Depending on the type of surface boundary condition, the large circulation reacts with a slow-down of overturning and gyre circulations. Restoring of the total or mean surface salinity prevents a large scale redistribution of the salinity field that is apparent under mixed boundary conditions and with the EBM. The control run under mixed boundary conditions exhibits large and unrealistic oscillations of the meridional overturning. Although the reaction to the fresh water flux anomaly is similar to the response with the EBM, mixed boundary conditions must thus be considered unreliable. With the EBM, the waters in the deep western boundary current initially become saltier and a new fresh water mass forms in the north-eastern North Atlantic in response to the fresh water flux anomaly around Greenland. After an accumulation period of several decades duration, this new North East Atlantic Intermediate Water spreads towards the western boundary and opens a new southward pathway at intermediate depths along the western boundary for the fresh waters of high northern latitudes.

Keywords: Ocean circulation; Thermohaline circulation; Fresh water flux; Ice sheet mass balance

1. Motivation and background

Most coupled climate models agree that the thermohaline circulation will slow-down due to smaller meridional air temperature gradients and an increased fresh water input in high northern latitudes under increasing greenhouse gas concentrations in the atmosphere (Cubasch et al., 2001). However, the magnitude of the trend differs among models, the sensitivity of the ocean component being one candidate for this uncertainty. This

* Corresponding author.
E-mail address: rgerdes@awi-bremerhaven.de (R. Gerdes).

1463-5003/$ - see front matter © 2005 Elsevier Ltd. All rights reserved.
doi:10.1016/j.ocemod.2005.08.003

situation motivated the Coupled Model Intercomparison Project (CMIP) to launch coupled experiments where the oceanic component was supplied with an additional fresh water flux in the North Atlantic (Stouffer et al., in press; www-pcmdi.llnl.gov/projects/cmip/coord_expt.html). It is desirable to conduct corresponding experiments with ocean–sea ice models where atmospheric conditions can be prescribed, allowing one to study the effects of anomalous fresh water fluxes in isolation. Additionally, more detailed ocean models can be utilized than currently used in coupled climate models and parameterizations and other model choices can be varied at smaller computational expense.

Among the possible sources of additional fresh water input to the North Atlantic are an enhanced hydrological cycle, the depletion of the Arctic sea ice and fresh water reservoirs, and enhanced melt water flux from Greenland. An enhanced hydrological cycle implies more precipitation over the catchment area of the large Siberian rivers that drain into the Arctic Ocean (Peterson et al., 2002). The Arctic sea ice volume has been observed (Rothrock et al., 1999) and modelled (Holloway and Sou, 2002; Köberle and Gerdes, 2003) to decrease by a substantial fraction since its maximum in the mid-1960s. Enhanced melting of the Greenland ice sheet has been modelled for the IPCC96 IS92a scenario by Huybrechts and de Wolde (1999). They estimate that by the year 2500, the Greenland ice sheet could loose as much as a third of its volume.

In equilibrium, the ocean transports fresh water meridionally to compensate for the atmospheric transport. In most ocean basins this transport is achieved in gyre circulations where salty water is transported from the subtropics to higher and lower latitudes in western boundary currents and relatively fresh water is transported in the interior recirculations. The North Atlantic differs because it has the capability to transport fresh water to depths. Currently, the Labrador Sea Water receives a large amount of fresh water from the Arctic Ocean and partly the Pacific (through the Bering Strait). This fresh water is carried all the way to the Southern Hemisphere.

What happens when this capability to transport fresh water into the deep ocean is compromised by additional input of fresh water into the northern North Atlantic? This is the underlying question we wish to answer with 'water hosing' experiments as were conducted in the CMIP framework.

Although the estimates for changes in Greenland run-off vary and the changes over the current century might be small, we perceive a need to investigate the impact of substantial melt water fluxes from Greenland on the sea ice conditions in the Nordic Seas and the Labrador Sea, the deep water formation areas of the northern North Atlantic, the large scale oceanic circulation, and the oceanic heat transport which may all be immediately affected by the fresh water input. This problem poses a test for the ocean components of IPCC class coupled models and this has prompted the CLIVAR Working Group for Ocean Model Development (WGOMD) to include a protocol for so called 'water hosing' experiments in their suite of coordinated ocean-ice reference experiments (CORE; for details see http://www.clivar.org/organization/wgomd). Among the properties of ocean models to be tested in this context are the handling of a rather localized input of fresh water and the variation of sensitivity of the large scale circulation with the type of surface boundary conditions. What kind of surface boundary conditions should we use to most closely emulate the response in the coupled system—without losing the ability to essentially prescribe the atmospheric conditions?

It is well known that the large scale ocean circulation depends sensitively on the surface boundary conditions, i.e. the representation of the atmosphere in ocean–sea ice models. It is not clear how to overcome this dependency and to realistically represent the most important feedbacks that occur with an active atmosphere. After introducing the model and the atmospheric forcing fields in Section 2, the experimental design in Section 3, we will, in Section 4, present results from water hosing experiments where we use different surface boundary conditions for salinity, ranging from simple restoring of surface salinity to prescribed fluxes combined with an energy balance model. We summarize our findings in Section 5.

2. Model and forcing

The ocean–sea ice model uses version 4 of the Modular Ocean Model (MOM4) of the Geophysical Fluid Dynamics Laboratory (GFDL). The sea ice model is the Sea Ice Simulator (SIS) of Winton (2000). Some experiments use an energy balance model (EBM) for the atmosphere. This component is described in Russel et al. (2005). With the EBM the land surface model LM2 (GFDL Global Atmospheric Model Development Team, 2004) is used. The EBM is a simple spectral atmospheric model using uniform diffusion and a radiative

balance. It solves prognostic equations for atmospheric temperature and specific humidity. The wind field is specified from data and not calculated by the EBM. The equation for the atmospheric temperature tendency includes the balance of shortwave and longwave radiation terms at the surface. It does not include effects due to water vapour, other than the latent heat flux released during precipitation. The specific humidity is calculated as the balance between evaporation and both liquid and frozen precipitation. For simplicity several properties (albedo, glacier location and mass) have been prescribed that are usually predicted. Although the EBM carries moisture, precipitation is taken from data (see below). In addition, the vegetation and soil type used are constant everywhere. All model components are coupled via the GFDL Flexible Modelling System (FMS). A description of the ocean model in its OM3 configuration and a rationale for different choices of grid design, numerical algorithms, and parameterizations can be found in Griffies et al. (2005). Gnanadesikan et al. (in press) discuss its performance as part of the GFDL coupled climate model.

Here we use the model in the similar but somewhat coarser resolution OM2 configuration. OM2 has a spherical Mercator grid with 2° resolution in the zonal direction and $2°\cos\phi$ in the meridional direction south of $\phi = 65°$N. At 65° latitude the resolution is thus around 100 km. The grid also features a factor three equatorial refinement in meridional resolution to improve the representation of equatorial waves and the equatorial current system. North of 65°N the grid switches to a bipolar region (Murray, 1996), with poles over Siberia and Canada. Details of this transformation are given in Griffies et al. (2004).

The model contains 50 vertical levels, the 22 uppermost levels are equidistant with 10 m spacing, the lower 28 increase in thickness such that the maximum depth becomes 5500 m. Partial bottom cells (Pacanowski and Gnanadesikan, 1998) are employed to better represent especially the gentle bottom slopes of the large abyssal basins. The topography is discretized from a dataset assembled at the Southampton Oceanography Centre (Andrew Coward, personal communication) and blends the Smith and Sandwell (1997) atlas with the IBACO atlas (Jakobssen et al., 2000) and the ETOPO5 data set (NOAA, 1988). Modifications to ensure proper flow through passages were made in Denmark Strait, the Iceland–Scotland Ridge system, the Carribean, and the Indonesian Archipelago. The resulting model topography is shown in Fig. 1. The Mediterranean and other marginal seas are not directly connected with the large ocean basins. Exchanges between marginal seas and the ocean basins are achieved with the cross-land mixing scheme described in Griffies et al. (2004). An additional exchange of volume happens at a rate proportional to the difference in surface height between the basins to avoid drying up of the uppermost cell in evaporative sub-basins. A bottom-boundary layer parameterization according to Beckmann and Döscher (1997) is included to improve the representation of dense overflows. Transports within this boundary layer are diffusive in our implementation.

The free surface method of Griffies et al. (2001) is used in OM2. It allows the direct flux of fresh water through the surface and thus an ocean volume that changes with time. There is no need for virtual fluxes of salt or other tracers. This is of some importance in the water hosing experiments to be discussed below.

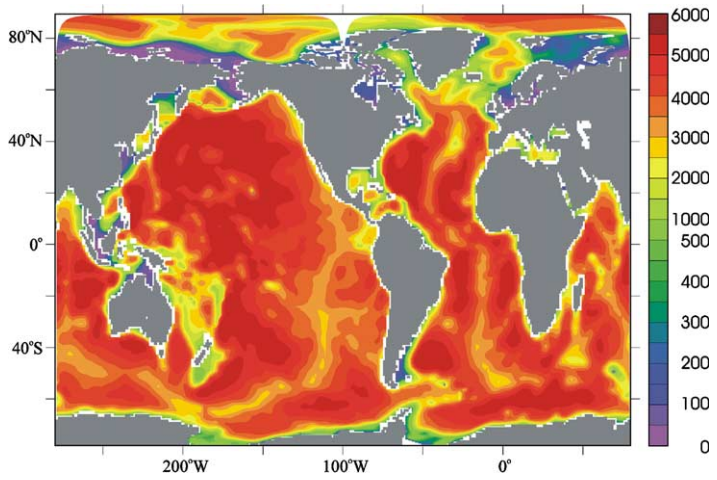

Fig. 1. Depth (in m) at tracer grid points. Note the different shading intervals for depths below and above 500 m.

To avoid an otherwise possible vanishing of the uppermost ocean layer (nominal thickness of 10 m), the pressure from sea ice felt by the ocean surface is restricted to that of 4 m thick ice. This does not affect the properties of the ice itself which can grow thicker than this threshold; mass exchanges between ocean and sea ice are properly taken care of.

Advection of tracers is handled by a third order upwind biased approach (Hundsdorfer and Trompert, 1994) with flux limiters according to Sweby (1984) that ensure that tracers do not exceed their natural bounds.

Neutral physics are implemented following Griffies et al. (1998) and Griffies (1998). The diffusivity along neutral surfaces is the same depth-independent function of the flow as the skew-diffusivity that governs the eddy induced velocity, $\mathbf{u}^* = -\delta_z(\kappa \mathbf{S})$ where $\mathbf{S}$ denotes the slope of the neutral surface. The diffusivity is set proportional to the baroclinicity vertically averaged between 100 m and 2000 m depth. Upper and lower bounds of 600 and 100 $m^2\ s^{-1}$, respectively, are imposed. In regions of strongly sloping neutral surfaces, neutral diffusivity is exponentially converted to horizontal diffusion (Large et al., 1997). The layer in which this tapering occurs is the neutral boundary layer. In the neutral boundary layer, the skew-diffusivity is set such that the eddy induced velocity is constant with depth (Griffies, 2004). Neutral physics reverts to horizontal diffusion when truncation errors cause tracer values outside their physical range and adjacent to all boundaries.

Outside the tropics, viscosity is composed of a grid size dependent and vertically constant background viscosity added to a horizontal shear dependent Smagorinsky viscosity (Smagorinsky, 1963; Griffies and Hallberg, 2000). The shear dependent contribution is important in the western boundary currents but is sub-dominant to the background viscosity otherwise. The isotropic part of the viscosity is reduced by 2/3 poleward of 60°N to suppress a coupled ocean and sea ice instability associated with frictional CFL violation. Inside 20° latitude, the viscosity is anisotropic according to the methods of Large et al. (2001) and Smith and McWilliams (2003). Here, we use a zonal viscosity component larger than the meridional component by a factor as much as 50 near the equator. Consistent with the results of Large et al. (2001), the anisotropic viscosity scheme allows an equatorial current system of realistic strength while still suppressing numerical noise as needed. Vertical viscosity is set to $10^{-4}\ m^2\ s^{-1}$ throughout.

For the simulation of the surface mixed layer the KPP scheme of Large et al. (1994) is used. In the computation of the Richardson number, a contribution from unresolved tidal motion is taken into account. This shear is taken from a tide model according to Lee et al. (2006). In addition, double-diffusive mixing and convective adjustment as well as a Bryan and Lewis (1979) vertical dependence of diapycnal diffusivities are implemented. The Bryan and Lewis coefficients are constant in time and vary in the upper levels from $10^{-5}\ m^2\ s^{-1}$ in the tropics to $3 \times 10^{-5}\ m^2\ s^{-1}$ in high latitudes. At depth, the coefficient increases to $1.2 \times 10^{-4}\ m^2\ s^{-1}$ everywhere.

Heat and momentum fluxes at the ocean or sea ice surface are calculated using bulk formula. Atmospheric data are taken from Röske (2001). This data set contains monthly mean fields over the ERA15 reanalysis period 1979–1993. The monthly means are augmented by daily variability that is taken from a selected year (1982). Daily variability was considered essential for realistic surface fluxes. It is repeated each year of the ocean model integration. The choice of the particular year for the daily variability is motivated in Röske (2006). As with any particular year, the synoptic atmospheric variability of the El Niño year 1982 might influence highly nonlinear processes like deep convection in the northern North Atlantic.

The Röske (2001) data include river run-off which is inserted into the ocean model as described by Griffies et al. (2005). The procedure tries to avoid unrealistically low salinities near the surface by distributing the run-off over the upper four model grid cells. The surface height reflects the added volume of water as if all of it had been inserted in the uppermost grid-cell. In addition, enhanced mixing is applied near the river mouths. The tidal mixing scheme contributes to the spreading of river water because high shears are present over the shallow shelves where many rivers enter the model. Absorption of solar radiation is regulated by chlorophyll concentration taken from the climatology of Sweeney et al. (2005). This allows heating of layers below the immediate surface layer especially in the clear waters of the subtropical oceans.

Although the averaging period for the atmospheric data is biased towards positive NAO states, it turned out that heat losses in the Labrador Sea were too small to sustain deep convection there. The meridional overturning circulation in the Atlantic slowed to an unacceptable value. To reproduce a realistic meridional overturning, the scalar wind was enhanced only in the Labrador Sea by a factor with a spatial distribution of $1 + 0.3 * (1 + \cos(\pi r/1500))$ where r is the distance (in km) from the centre of the Labrador Sea at 58°N, 57°W. There is no change in the scalar wind outside the region of the Labrador Sea ($r > 1500$). Note that this

measure only affects the rate of heat exchange between ocean and atmosphere but does not prescribe surface density in the Labrador Sea.

Surface fresh water fluxes are due to prescribed precipitation (from Röske, 2001), evaporation from bulk formula, melting and freezing of sea ice, and prescribed run-off. In some experiments, surface salinity is additionally restored towards climatological annual mean values taken from Steele et al. (2001). The time scale is 60 days for an uppermost box of 10 m thickness. The restoring term is adjusted at each model time step by a globally uniform shift such that salt is conserved globally.

3. The experiments

The suite of experiments (Fig. 2) consists of two spin-up calculations of 100 years duration that are continued as control integrations for another 100 years (CONTROL and EBM-CONTROL). These spin-up runs start from rest and the Steele et al. (2001) climatology. After the spin-up, four experiments (RESTOR, SPLIT, MIXED, and EBM) and another control integration (MIXED-CONTROL) are started. The experiments are distinguished from the control integrations by an active fresh water flux anomaly that is applied over the whole duration of the experiments.

One can anticipate that several fresh water fluxes (strengthened hydrological cycle, reduction of Arctic sea ice and liquid fresh water reservoirs, and melt water from Greenland) will all lead to increased fresh water content in the boundary currents around Greenland. Models that aim at simulating these possible future developments must be able to cope with fresh water flux anomalies that are concentrated in these boundary currents. In our experiments we therefore deviate from the CMIP design where the fresh water flux anomaly was distributed over the latitude band 50°N–70°N in the North Atlantic. The latter choice was partly motivated by numerical considerations that are less compelling in the case of ocean-only models. Here, the fresh water flux anomaly (fwf) is distributed along the eastern and western coasts of Greenland between the southern tip of Greenland and Fram Strait on the eastern side and between the southern tip of Greenland and the southern end of Nares Strait at approximately 76°N on the western side (Fig. 3),

$$\begin{aligned} \mathrm{fwf} &= \alpha \mathrm{e}^{-x/x_{\max}} && \text{for } x \leqslant x_{\max} \\ \mathrm{fwf} &= 0 && \text{for } x > x_{\max} \end{aligned}$$

where x is the outward distance perpendicular from the Greenland coast, $x_{\max} = 300$ km. The coefficient α is used to adjust the amount of integrated fresh water flux anomaly to 0.1 Sv,

$$\alpha = \frac{0.1\ \mathrm{Sv}}{\int_A \mathrm{e}^{-x/x_{\max}}\,\mathrm{d}A}$$

where A is the area of those grid cells where fwf $\neq 0$.

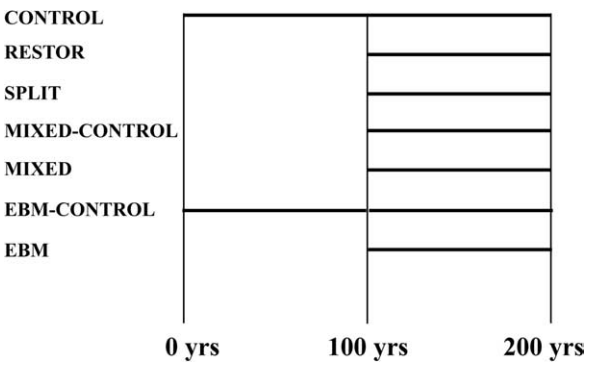

Fig. 2. Experimental design: Spin-up integrations (CONTROL, EBM-CONTROL) start at year 0 and are continued for 100 years. They provide initial conditions for control integrations and experiments which are performed for years 101–200. Experiments differ from the corresponding control integration by an additional fresh water flux around Greenland (see Fig. 3).

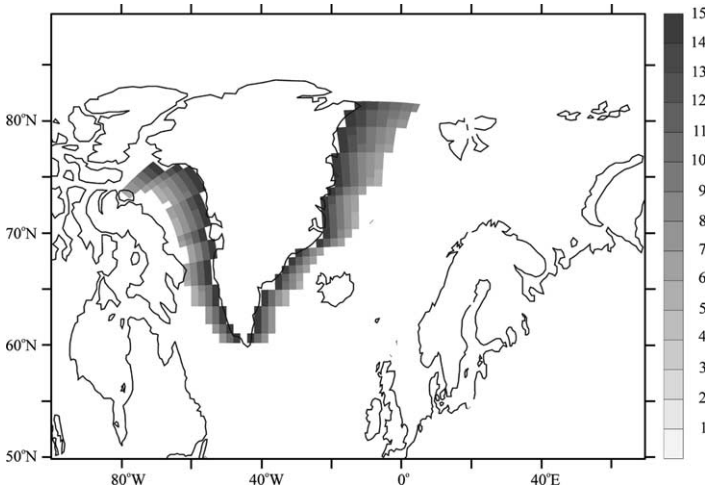

Fig. 3. Surface fresh water flux anomaly in m/yr.

We consider the fresh water flux anomaly around Greenland as more realistic than the broad water hosing of CMIP because it better reflects the distribution of expected additional future fresh water input into the northern North Atlantic. The distribution of the fresh water flux anomaly and especially its relation to the downward pathways of the meridional overturning circulation in the Atlantic are important for the transient response of the ocean.

In all model runs, the total fresh water flux integrated over the global ocean was kept at zero by compensating any imbalance with a globally uniform fresh water flux correction. The anomalous fresh water input around Greenland is slightly higher than the average increased melt rate over the next 500 years estimated by Huybrechts and de Wolde (1999) for the Greenland ice sheet. It should be noted that the melt water flux from Greenland is not expected to be constant in time as is assumed here.

The length of the experiments is chosen as 100 years because major advective adjustments took place only after several decades into the integration. The assumption of a static atmosphere is not valid over such a period. However, the proposed experiment is not primarily designed to realistically describe the climate system's reaction to increased melting of the Greenland ice sheet. The primary purpose is to study the sensitivity of ocean general circulation models (OGCMs) and the adjustment processes in response to a certain fresh water flux perturbation without the complication of changes in other forcing fields. An active atmosphere is used to calculate air temperature, however, in the EBM experiment. Still, many feedbacks possible in a fully coupled system are ignored there.

We expect that the oceanic response depends on the surface boundary conditions for salinity. Here we have used four different approaches. The boundary conditions vary from the classical restoring of surface values to climatology as described above (RESTOR), mixed boundary conditions where the total fresh water flux is prescribed (MIXED), and a method where the salinity consists of two parts of which only one is restored to climatology while an "anomaly" part receives the anomalous fresh water flux and is not damped (SPLIT). The fourth approach is to use a coupled atmospheric EBM-ocean–sea ice model (EBM). All experiments and control runs carry a tracer S_1 that represents a salinity anomaly due to the anomalous fresh water flux. In the SPLIT experiment this tracer is dynamically active, otherwise it is passive and used for diagnostic purposes. To avoid a jump in the boundary conditions at the end of the spin-up, the MIXED and EBM experiments are forced with an additional fresh water flux equivalent to the restoring term, derived from an average over the last 20 years of the corresponding spin-up integration.

The SPLIT experiment is intended to provide an alternative boundary condition for salinity that allows fresh water anomalies to develop freely and not be damped away by a restoring term on surface salinity. This is achieved by splitting the salinity into two active components S_0 and S_1 which feel different surface boundary conditions. The conservation equations are

$$\frac{\partial S_0}{\partial t} + \nabla \cdot (\mathbf{u} S_0) = D(S_0) + \gamma(S^* - S_0)$$
$$\frac{\partial S_1}{\partial t} + \nabla \cdot (\mathbf{u} S_1) = D(S_1)$$

and the equation of state is calculated with the total salinity $S_0 + S_1$. S_0 and S_1 are subject to the same advection and subgrid scale operators (D) while only S_0 is restored towards a climatology S^*. Like all other tracers, S_0 and S_1 are affected by the volume changes associated with surface fresh water fluxes. It is not possible to introduce a surface fresh water flux anomaly without affecting both tracers, contrary to our intention in this experiment. Therefore, we apply the anomalous surface flux fwf as an equivalent salt flux fwf $(S_0 + S_1)$ to the S_1 field. The local surface salinity is used in this transformation for higher accuracy and to prevent unrealistic (e.g. negative) surface salinities. Note that due to this different treatment of the anomalous fresh water flux, the SPLIT experiment experiences a slightly different forcing than the other experiments of this suite. In all other runs the tracer S_1 is purely diagnostic.

4. Results

4.1. Control integration

To judge the quality of the control integration under surface salinity restoring we consider the following diagnostics: the deviation from climatology of salinity at 100 m and 2000 m depth at the end of the integration, the meridional overturning in the Atlantic, meridional heat transports, and volume transports through several choke points of the global circulation.

Potential temperature at 100 m depth (Fig. 4) shows largest deviations from climatology in the tropical Pacific and Atlantic as well as in the northern North Atlantic. The latter are associated with the Gulf Stream path that is too far north as is the case in most models of this resolution. Overly large heat losses in the boundary current off the North American continent are the reason for too little heat transport divergence in the subpolar Atlantic and the Nordic Seas. The tropical biases can be attributed to a too thick thermocline in the eastern parts of the basins.

Similar biases due to the shift in the Gulf Stream position exist in the North Atlantic at depths to 1000 m. At these depths we see an increasing warm bias of the Nordic Seas, contrary to the near surface layers. This warming is caused by the lack of efficient heat release from the Atlantic layer under a strong halocline. Climatological data show near freezing temperatures in the deep basin of the Nordic Seas. These cold waters spread from the deep convection site in the Greenland Sea into the Norwegian Sea and into the Eurasian Basin (Bönisch and Schlosser, 1995). Convection in the Greenland Sea is often associated with freezing of sea ice (Marshall and Schott, 1999; Gerdes et al., 2005) and temperatures are thus close to the freezing point. In the model, the Greenland Sea and relatively large parts of the Barents Sea are covered with sea ice and a thick layer of fresh water that prevent deep convection and cooling at deeper levels in both areas. Except for small parts of the Siberian shelves, the Arctic Ocean and the Greenland Sea experience no effective surface cooling in the model. The inflowing Atlantic Water thus slowly warms the whole area, leading to the excessive thickness of the Atlantic layer in the Arctic Ocean and the too high temperature and areal extent of the return Atlantic Water in the western Nordic Seas. Consequently, with above 3 °C the Denmark Strait Overflow Water (DSOW) in the model is far too warm. Density is less affected (reaching $\sigma_0 = 27.9$ at the sill) because the return Atlantic Water is also too saline.

Temperature biases at 2000 m depth (Fig. 5) are thus dominated by a too warm overflow from the Nordic Seas into the sub-polar North Atlantic. Effective cooling by deep Labrador Sea convection results nevertheless in a deep western boundary current (DWBC) that is slightly too cool. Locally, large discrepancies exist in the Southern Ocean, most of them associated with deviations of the frontal positions in the model from those observed.

The passive tracer S_1 is forced like in the experiments as if a fresh water flux anomaly around Greenland were present. The resulting Atlantic distribution at 100 m and 2000 m depth are shown in Fig. 6. Since this tracer is incorporated in the boundary currents around Greenland, it effectively traces the pathways of near

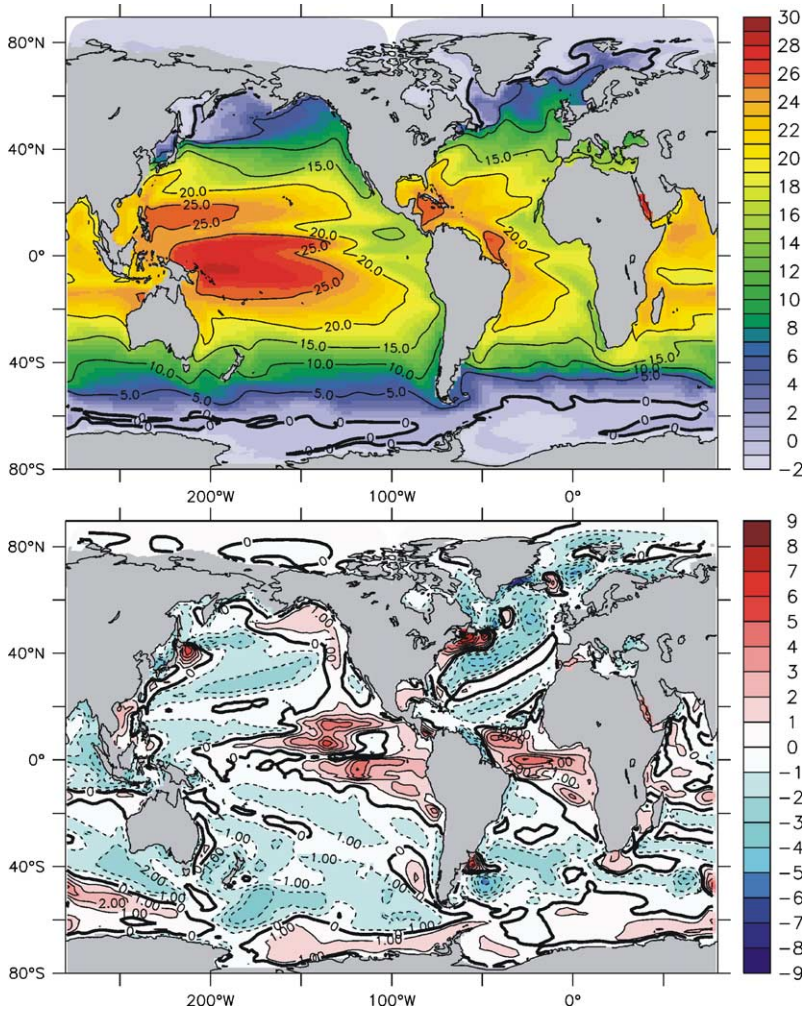

Fig. 4. Potential temperature at 100 m depth averaged over the last 20 years of the CONTROL run (top), and deviation from annual mean climatology (bottom).

surface waters of Arctic Ocean origin. Fig. 6(left) reveals that this water stays near the surface only to the southern end of the Labrador Sea. It is restricted to the EGC and the boundary currents of the Labrador Sea. Before this water can reach further south, it is carried to depths, either by convective mixing or more likely by strong vertical advection along the rim of the Labrador Sea, the most important downward branch of the Atlantic meridional overturning circulation in the model. At 2000 m (Fig. 6(right)), the tracer can be followed along the very distinct DWBC into the Southern Ocean where it is carried eastward. Within 100 years since the beginning of tracer release around Greenland, the tracer has reached the southern parts of the eastern Pacific.

The strength of the meridional overturning increases during the control run from 13 Sv at the end of the spin-up to 18 Sv at the end of the run. Only 4 Sv upwell within the Atlantic such that the exchange rate with the Southern Ocean is 14 Sv at the end of the run. With the intensification of the overturning, we find increasing convective activity in the northern North Atlantic (Fig. 7) that stabilizes at a relatively high level towards the end of the integration. Convection depths in the Labrador Sea reach 2500 m. Mixed layer depths of more than 1000 m are also found in the Irminger Sea. There is no convection exceeding 200 m in the Nordic Seas except for the eastern rim that is affected by the Norwegian-Atlantic Current.

Transports through certain key passages are listed in Table 1. There is a net flow from the Atlantic into the Nordic Seas between Iceland and Scotland of 7.4Sv which is balanced by a corresponding outflow from the

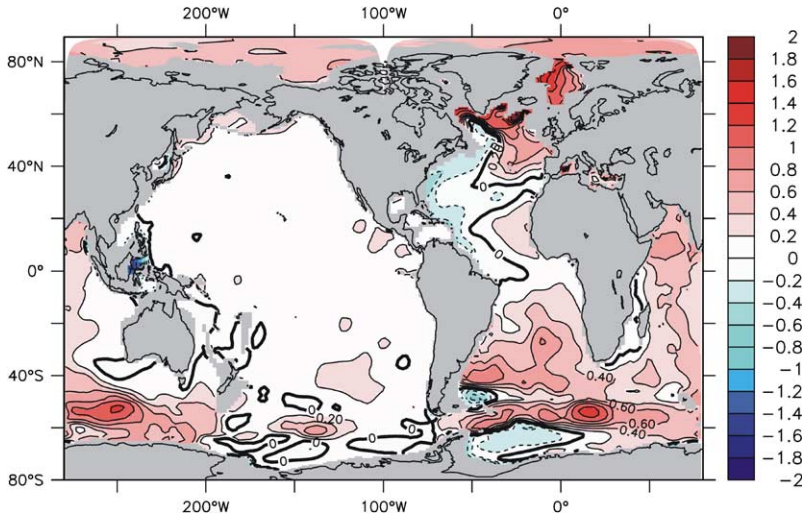

Fig. 5. Deviation of simulated potential temperature at 2000 m depth averaged over the last 20 years of the CONTROL run from annual mean climatology.

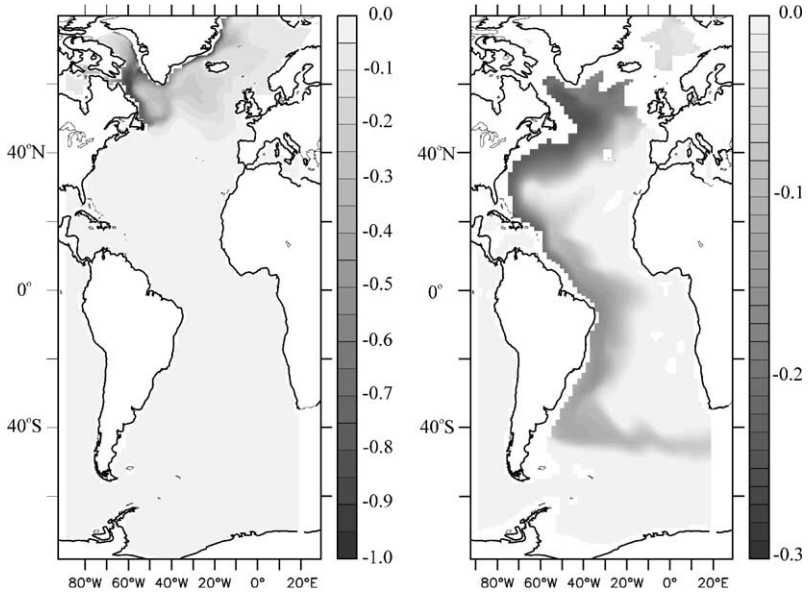

Fig. 6. Passive tracer S_1 at 100 m depth (left) and at 2000 m depth (right) averaged over the last 20 years of the CONTROL run. The tracer is forced by a flux similar to that used in the experiments where it is active, however.

Nordic Seas into the sub-arctic North Atlantic through Denmark Strait. This indicates that the magnitude of the transport from the Pacific into the Arctic Ocean through Bering Strait (0.9 Sv in the model) is equal to that through the Canadian Archipelago. The exchange rates between the Nordic Seas and the North Atlantic are high compared to available estimates based on observations. The reason is that inflow and outflow are differently distributed among the straits compared to nature. There is virtually no deep outflow to the North Atlantic through the Iceland–Scotland gap. Instead, all the outflow from the Nordic Seas is channelled through the Denmark Strait.

The observed Gulf Stream transport at 27°N and the flow through the Indonesian Archipelago are reasonably well reproduced in the model. The ACC transport at Drake Passage is roughly 30 Sv higher than the

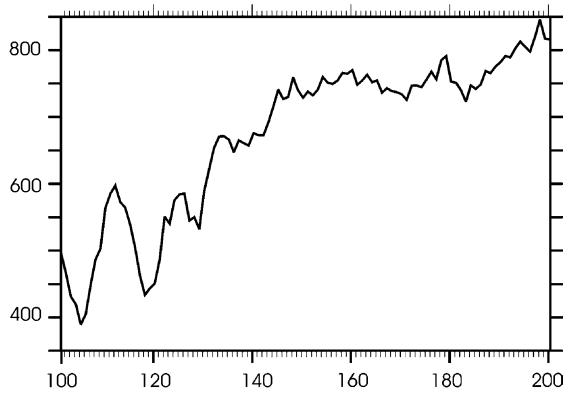

Fig. 7. Time series of March through May mixed layer depth (in m) in the control run averaged over the area 50°N–60°N, 60°W–40°W (approximately the Labrador Sea).

Table 1
Transports through key locations

	CONTROL	EBM-CONTROL	RESTOR	SPLIT	MIXED	EBM	OBS
MOC_{Atl}	17.5	16.4	13.6	15.9	6.5	8.9	18
Gulf Stream 27°N	35.0	38.5	30.5	38.2	24.0	28.5	28.7–34.7
Denmark Strait	−7.4	−8.6	−7.8	−8.3	−6.8	−4.2	−3.3/−5.0
Iceland–Scotland	7.4	7.7	7.3	8.1	6.8	3.7	4.3
Drake Passage	167.5	153.4	169.0	165.4	168.0	159.5	134
Indonesian Archipelago	−9.2	−9.5	−7.9	−8.8	−7.2	−7.5	−10
Bering Strait	0.9	1.5	0.9	1.0	0.3	0.8	0.8

MOC_{Atl} denotes the maximum overturning in the NADW cell of the Atlantic. Indonesian Archipelago denotes the total transport from the Pacific into the Indian Ocean between the Asian continent and Australia. All values are vertically integrated net transports given in Sv. They are diagnosed from the velocity field averaged over years 181 through 200. Negative values are for southward and westward flows. Observational estimates are taken from Cunnigham et al. (2003) (Drake Passage), Gordon et al. (2003) (Indonesian Archipelago), Leaman et al. (1987) (Gulfstream at 27°N), Roach et al. (1995) (Bering Strait), Hansen and Østerhus (2000) (Iceland–Scotland and Denmark Strait). The uncertainty in the Denmark Strait transport stems from the unknown outflow of near surface waters. The range is derived using continuity and an upper bound of flow through the Canadian Archipelago of 1.7 Sv.

Cunnigham et al. (2003) estimate. This can be regarded as satisfactory because the ACC transport is very sensitive to relatively small changes in the atmospheric forcing.

The maximum global heat transport is 1.3 PW (at 15–20°N), somewhat lower than the 1.8 PW estimated for the real ocean (Fig. 8). Most of this heat transport is achieved in the North Atlantic where the maximum is 0.9 PW in the model. Whereas the heat transport in the North Atlantic reproduces the estimates relatively well, somewhat larger differences occur in the Southern Hemisphere where the model considerably underestimates the heat transports.

4.2. Control integration with EBM

Since there is less direct forcing towards realistic surface temperatures and salinities in the control run with the atmospheric EBM, the biases in this simulation are expected to be larger than in the above control run. Deviations from climatology are larger in EBM-CONTROL than in CONTROL in the north-western North Atlantic and the northern North Pacific as well as in the eastern tropical Pacific (Fig. 9). Overall, the potential temperature at 100 m depth has a warm bias. The air temperature predicted by the coupled system is much more zonally symmetric than observed, resulting in too high temperatures over the north-western North Atlantic while the eastern parts are somewhat too cold. Nevertheless, the model is able to produce a vigorous inflow of Atlantic water into the Nordic Seas (Table 1). As in CONTROL, the deep Nordic Seas become too warm because of a too intense halocline and the lack of deep convection. Deep convection occurs in the model

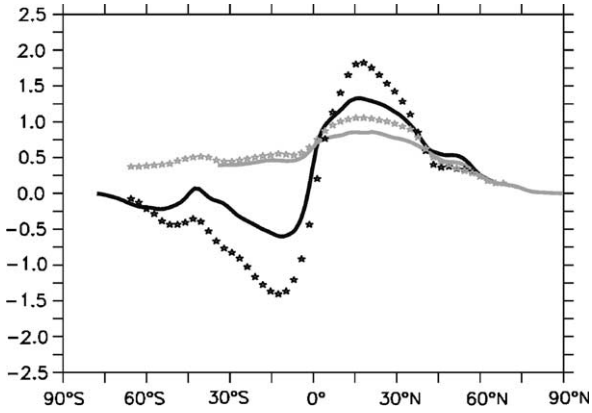

Fig. 8. Total global heat transport (black) and the contribution from the Atlantic (grey) in the model averaged over the last 20 years of the CONTROL run. Estimates for the real ocean from Trenberth and Caron (2001) are given by the corresponding stars.

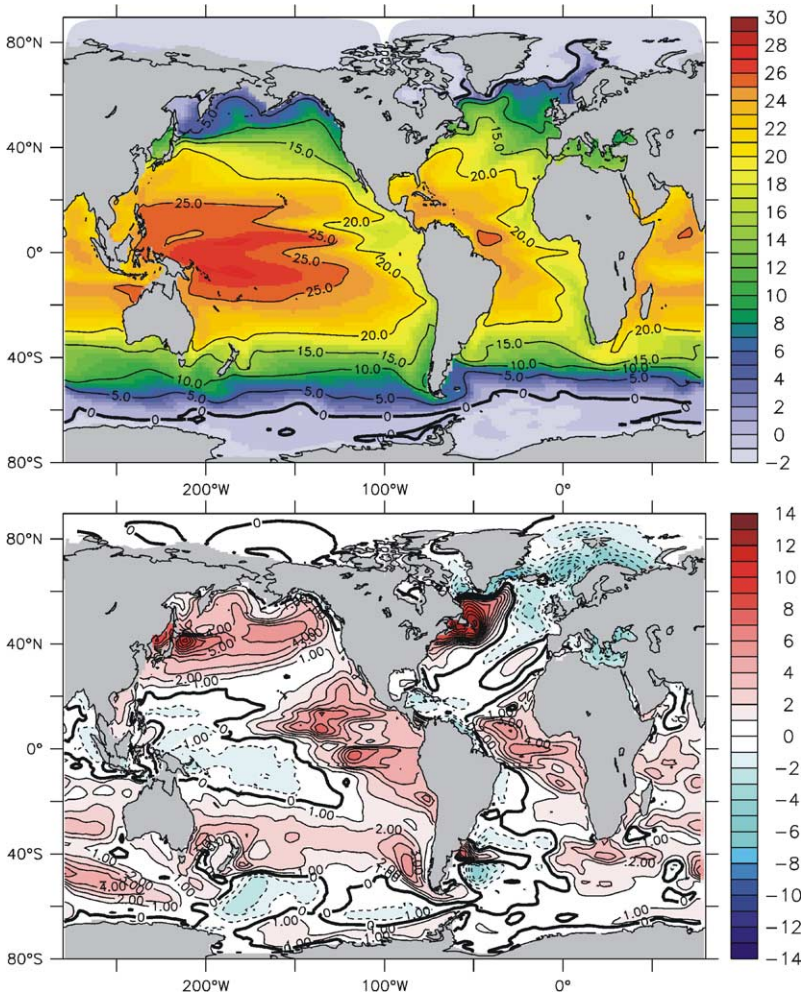

Fig. 9. Potential temperature at 100 m depth averaged over the last 20 years of the EBM-CONTROL run (top), and deviation from annual mean climatology (bottom).

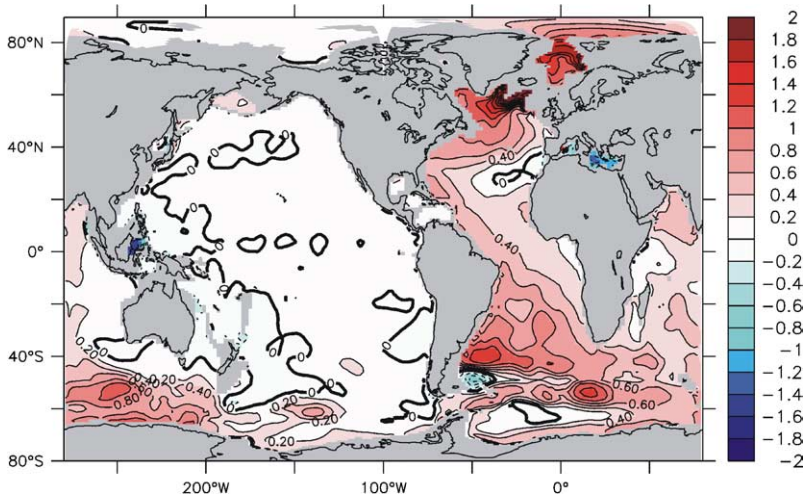

Fig. 10. Deviation of simulated potential temperature at 2000 m depth averaged over the last 20 years of the EBM-CONTROL run from annual mean climatology.

just south of Iceland. It brings very warm water down to 2000 m (Fig. 10). This is similar to the warm deep water flowing over the Greenland–Scotland Ridge in CONTROL. However, here it is of local origin and does not result from overflow of the Greenland–Scotland Ridge. In spite of the enhanced scalar winds over the Labrador Sea, no further deep convection sites exist in the northern North Atlantic. Thus, the DWBC and the deep South Atlantic become too warm in EBM-CONTROL.

Disregarding these differences in deep water formation, the strength (Table 1) and structure of the Atlantic overturning cell are very similar to CONTROL (see Fig. 12). Other key parameters of the flow are also similar between the two control runs. Correspondingly, the heat transport in the Atlantic is similar to CONTROL. The poleward heat transport in the southern Indian and Pacific are even smaller than in CONTROL, leading to a large discrepancy to observational estimates in the Southern Hemisphere.

The distribution of the passive tracer S_1 in EBM-CONTROL is very similar to the result of CONTROL with little of the tracer present near the surface while the bulk resides in a very well pronounced DWBC layer. The different location of deep sinking in the northern North Atlantic thus does not affect the downward and southward pathway of Arctic origin waters in any qualitative sense.

4.3. Reaction of meridional overturning and oceanic heat transport

The model ocean circulation is not in equilibrium with the forcing during the control integration as illustrated by the trends discussed above. However, certain features of the hydrography are well established although slow adjustments are still taking place. As will be shown below, changes in certain experiments far exceed the adjustments during the control integration and are clearly forced by the fresh water flux anomaly. Thus, we found it justified to compare perturbation experiments with control runs as well as final and initial states of experiments to identify the effect of the fresh water flux anomaly.

The strength of the deep meridional overturning (excluding the shallow cells that contain the zonally integrated Ekman transports as their upper limbs) is depicted in Fig. 11. The RESTOR and SPLIT experiments show a slight decline of the overturning compared to the CONTROL experiment. It is remarkable that SPLIT is less sensitive to the fresh water flux perturbation than RESTOR although the anomaly is not damped away as it is the case in RESTOR. EBM and MIXED exhibit a more pronounced drop in the strength of the overturning.

While the control runs CONTROL and EBM-CONTROL look similar and their overturning circulation increases gradually over the integration period, the corresponding control run under mixed boundary conditions exhibits large amplitude multi-decadal fluctuations of the overturning. These internal oscillations of the ocean–sea ice system are highly unrealistic since they would involve changes in oceanic transports and sea ice extent that have not been observed for the present climate. We have not investigated the cause of the oscillations

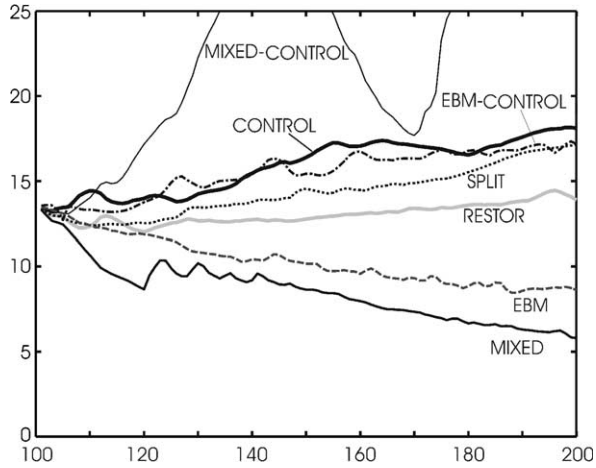

Fig. 11. Maximal strength (in Sv) of the NADW meridional overturning cell in the North Atlantic (see text) during the duration of the experiments. CONTROL: thick solid line; MIXED-CONTROL: thin solid line; EBM-CONTROL: dash-dotted; RESTOR: thick gray line; SPLIT: dotted; EBM: dashed; MIXED: solid line.

but it is apparent that they are connected to the positive salt advection feedback that is unchecked under mixed boundary conditions. The unrealistic behaviour of MIXED-CONTROL reinforces the notion that mixed boundary conditions are in general unsuitable for ocean-only model experiments. Obviously, the MIXED-CONTROL run cannot be used to identify forced changes in the MIXED experiment and we will use differences between the state at the end and the beginning of the MIXED experiment in further analysis.

The final overturning states of the EBM and MIXED experiments as well as the CONTROL and EBM-CONTROL (Fig. 12) show that the southward branch of the overturning cell in the experiments with fresh water flux anomaly shifts to around 1500 m depth while it is slightly below 2000 m in the control runs. The strength of the overturning has been reduced to around 8 Sv (EBM) and 5 Sv (MIXED) in the northern North Atlantic, respectively. The export rates across 30°S are somewhat larger, a sign of ongoing adjustment processes.

The experiments MIXED and EBM yield rather similar results as far as integrated quantities like meridional overturning and heat transport are concerned. The strength of the ACC is also little affected (Table 1). The details of the adjustment, however, differ considerably. As the meridional overturning slows down in EBM, the surface air temperature drops over large parts of the sub-arctic North Atlantic and especially over the Nordic Seas (Fig. 13). SAT is up to 4 K cooler in EBM over the Labrador Sea and up to 5 K cooler over the Norwegian Sea in the experiment compared to the control case. This behaviour is similar to that of coupled Atmosphere—Ocean GCMs. The cooling is caused by an expansion of the Arctic halocline to lower latitudes and the reduction of the northward oceanic heat transport. The exchanges between the sub-arctic Atlantic and the Nordic Seas in EBM are weakened much more than in other experiments (Table 1). Compared to the result of "water hosing" experiments of Manabe and Stouffer (2000) the response here is rather large over the Nordic Seas due to a southward advance of the sea ice. Since SST is more or less fixed by the prescribed surface air temperature in MIXED, no such changes in sea ice extent can occur in that experiment (Fig. 14). It should be noted that sea ice covers a larger part of the Nordic Seas and the Barents Sea in the EBM control run than in the control run under prescribed atmospheric forcing. However, the path of the Norwegian Atlantic Current is always ice free in the EBM control experiment.

The changes in sea ice in EBM have consequences for winter convection in the sub-polar Northwest-Atlantic as well as in the Nordic Seas. However, the strong convection in the sub-polar Northeast-Atlantic is only mildly affected. Convection there develops pronounced decadal scale oscillations during the experiment. Such oscillations were not present without the fresh water flux anomaly.

The SPLIT experiment was intended to provide an alternative boundary condition for salinity that would allow the fresh water anomaly to develop freely and not be damped away by a restoring term on surface salinity. Comparing surface salinity in SPLIT and RESTOR (not shown), this goal has been achieved. However,

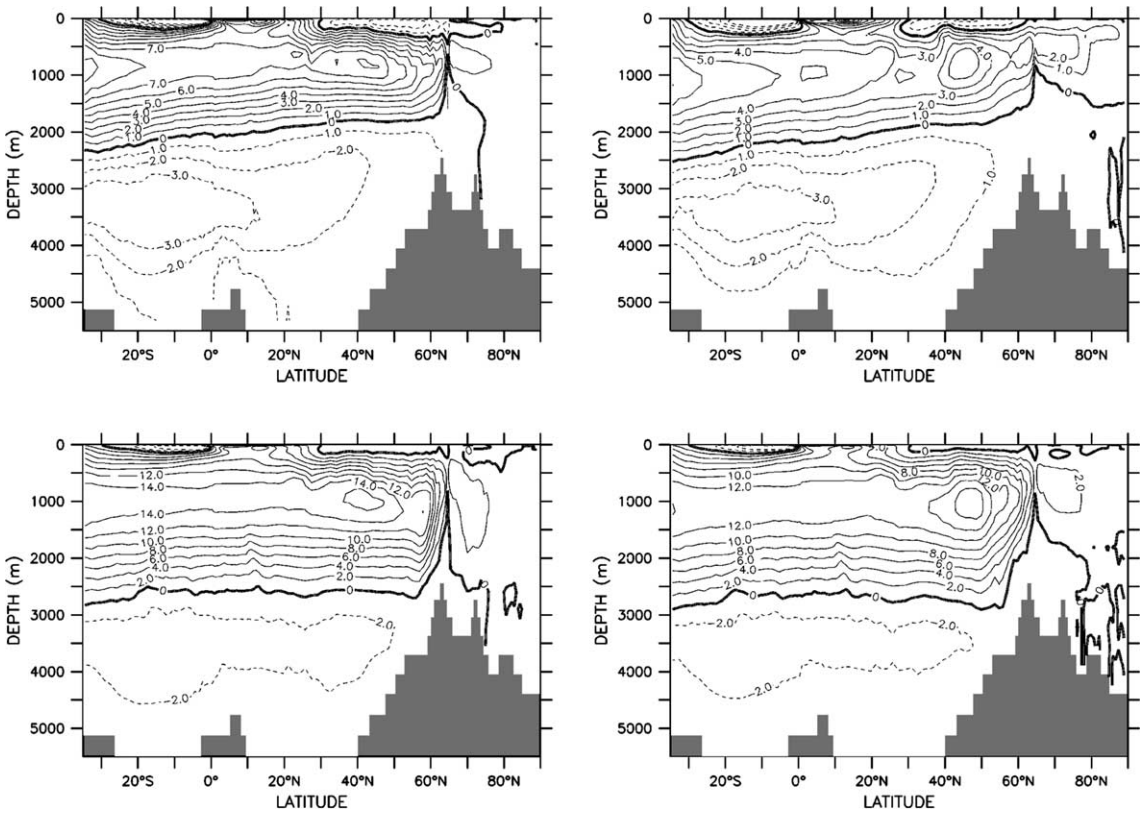

Fig. 12. Streamfunction of the zonally integrated volume transport in the Atlantic (in Sv). All maps represent averages over the last 20 years of the experiments. Upper left: EBM, upper right: MIXED, lower left: EBM-CONTROL, lower right: CONTROL. Note the different contour intervals for the experiments (1 Sv) and the control integrations (2 Sv).

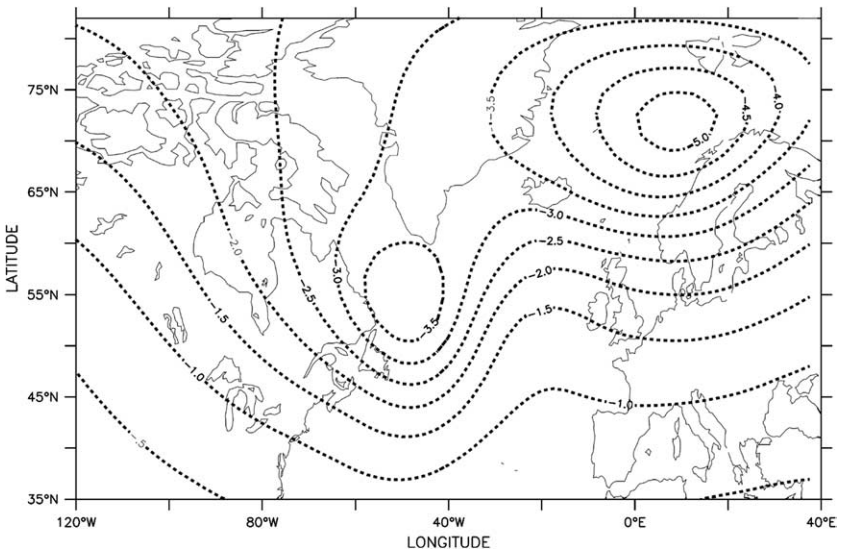

Fig. 13. Difference in surface air temperature between EBM and the corresponding control experiment. Contour interval is 0.5 K.

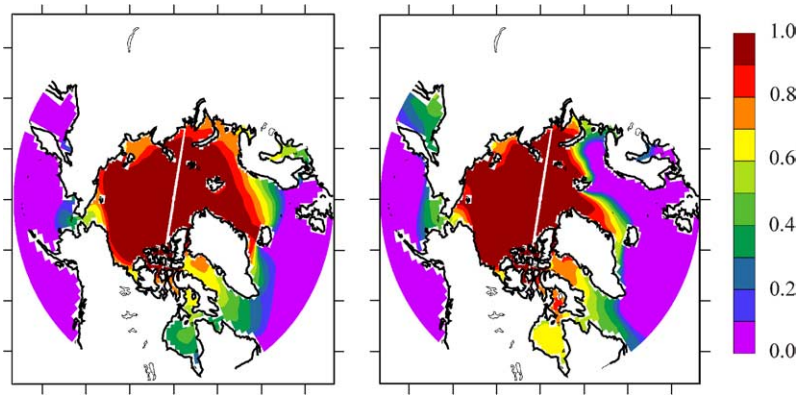

Fig. 14. Annual mean sea ice concentration averaged over the last 20 years of the experiments EBM (left) and MIXED (right). The contour interval is 10%.

the sensitivity of the large scale circulation with respect to the enhanced Greenland melt water flux is the lowest of all cases considered here, including the RESTOR case. The reason that the response is much smaller than in MIXED and EBM lies again in the salt-advection feedback (Rahmstorf et al., 1996) that is active in those cases but not in SPLIT. The changes in the large scale circulation initiated by the fresh water flux anomaly invoke much larger changes than are directly due to the fresh water flux anomaly (see Figs. 6 and 13).

Still, it is surprising that the model is less sensitive under the SPLIT boundary condition than with surface salinity restoring. One important difference lies in the treatment of fresh water fluxes in these experiments. In RESTOR and all other experiments except SPLIT the fresh water flux enters the ocean model as a volume flux that affects the uppermost grid box and sea level. Thus, a positive sea level height is generated near the coast of Greenland that enhances the strength of the EGC. In SPLIT, the fresh water flux is converted to a virtual salt flux and has no direct effect on sea level. However, SPLIT features a somewhat stronger EGC and the exchanges between the Nordic Seas and the Atlantic proper are more intense (Table 1). We hypothesise that the larger inflow of saline waters into the Nordic Seas is responsible for a more stable thermohaline circulation in SPLIT.

4.4. Development of salinity anomalies

In the first decades after switching on the anomalous fresh water flux around Greenland, the salinity in the upper NADW increases as the supply of relatively fresh Labrador Sea Water (LSW) is reduced and Mediterranean-influenced water spreads westward (Fig. 15). The age of the water in the upper parts of the deep western boundary current increases substantially because of the reduced inflow of relatively young LSW. However, a fresh intermediate water is formed in the North-eastern Atlantic. This water, here called NEAIW, occupies an increasingly larger area in the eastern North Atlantic and eventually spreads westward, reaching the western boundary at 25°N after 40 years into the integration of EBM (Fig. 16). No such arrival of fresher water can be seen in RESTOR (Fig. 16). In this experiment, no pool of extremely fresh water is formed in the north-eastern North Atlantic because of the damping of surface anomalies and the resulting lack of response in the large scale circulation. In EBM, the changes in surface fresh water flux result in accumulation of fresh water in the sub-polar gyre and the opening of a new southward fresh water pathway. In RESTOR, the balance between surface fluxes and meridional transports is closed instead by the additional source provided by the restoring term.

In Fig. 17 we present the vertical integral of the salinity anomaly at the end of the EBM experiment in comparison with the tracer S_1 distribution which highlights the importance of the changes in circulation. The salinity is reduced in large parts of the North Atlantic and the Arctic Ocean. Salinity in the subtropical recirculation drops as some of the fresh water is diverted into sub-polar mode waters. Positive salinity anomaly integrals still indicate the effect of the reduction in LSW supply along parts of the western boundary. This is the case although the direct effect of the surface fresh water flux anomaly, as measured by the S_1 integral, is actually to reduce the salinity along the western boundary. Although the meridional overturning circulation

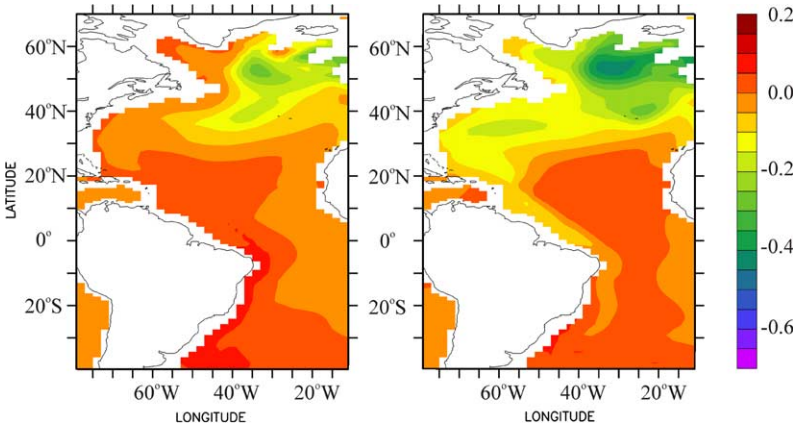

Fig. 15. Differences in salinity at 1500 m depth for EBM between 50 years (left) and 100 years (right) into the experiment and the initial conditions for the experiment.

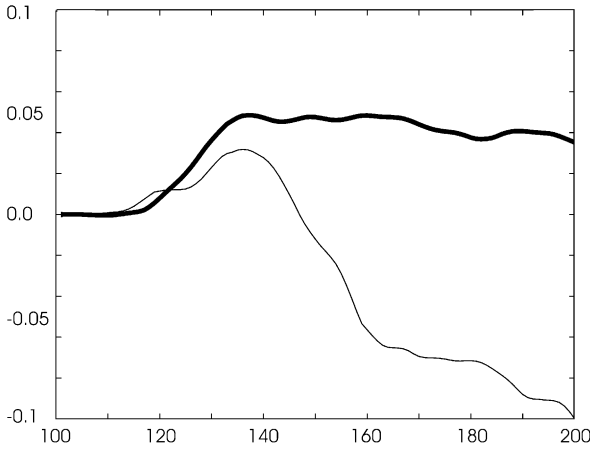

Fig. 16. Salinity anomaly (compared to control experiment) for LSW at 25°N. Salinity has been averaged between 75° and 65°W and then the minimum over the depth interval 0:5500 m has been taken. RESTOR: thick line; EBM: thin line.

slows down, it does not completely shut down in any of the experiments within the 100 years of the experiment. Thus, the salinity anomaly measured by the tracer S_1 follows the deep western boundary in the model's Atlantic. The signal has passed through the South Atlantic by year 100. The corresponding picture for the RESTOR experiment looks very similar (not shown) with somewhat higher concentrations in the western boundary and parts of the Southern Ocean. This reflects the advective time scale in the meridional overturning circulation that has become larger in the EBM experiment. The meridional overturning circulation itself responds on much faster time scales (Cessi et al., 2004), allowing the salinity field to develop substantial changes on a global scale.

In EBM, the indirect changes in salinity due to the weakening of the large scale circulation are far greater than the direct effect of the freshwater flux anomaly. The northern mid-latitudes of the Atlantic western boundary are already affected by the arrival of the NEAIW. The eastern part of the subtropical gyre of the North Atlantic is characterized by fresher mode waters. On the other hand, the South Atlantic has become more salty because of the reduced export to the North Atlantic. The same is true for most of the southern oceans where the export of saline water by the thermohaline circulation is reduced. The northern North Pacific is fresher because less fresh water is exported to the Arctic Ocean and also through the Indonesian Archipelago. The signature of AAIW and of reduced flow of relatively saline water around Southern Africa into the South Atlantic is visible. The Southern Ocean south of the ACC axis exports less fresh water to lower latitudes than in the control run.

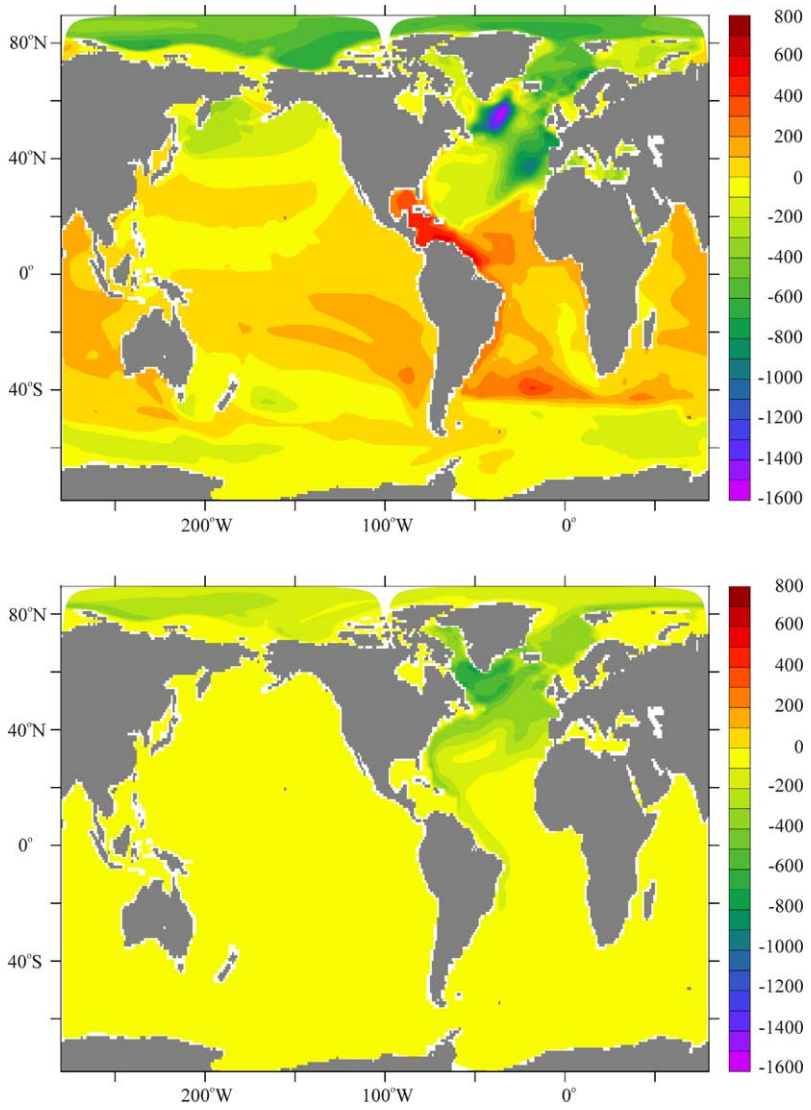

Fig. 17. Vertically integrated salinity anomaly (defined as the difference between the salinity at the end of the experiment and the end of the spin-up) for the EBM experiment (top) and the distribution of vertically integrated passive tracer S_1 at the end of that experiment (bottom). The units are m.

5. Summary

Forcing ocean–sea ice models with a fresh water flux anomaly around Greenland gives the opportunity to study the adjustment processes of the large scale oceanic circulation and the effect of the thermohaline circulation on the hydrographic state, sea level distribution, and heat transports. Our experiments show qualitatively similar results. This includes a weakening of convection in the Labrador Sea and of the strength of the DWBC. The DWBC shallows and initially carries more saline water than during the spin-up and the control experiments. The fresh water load is partly carried by southward moving subpolar mode waters.

Some features appear only in those experiments where the large scale circulation changes substantially in response to the anomalous fresh water input, namely the MIXED and EBM experiments. In both experiments without a restoring to surface salinity climatology we find global scale salinity anomalies, their magnitude far surpassing the anomaly directly induced by the imposed anomalous surface fluxes. Largest changes occur in

the North Atlantic and the Arctic. However, the effect of a weakened thermohaline circulation can be observed in an enhanced meridional salinity gradient in the Atlantic, a fresher North Pacific, and in the reduced exchanges between the Southern Ocean and southern mid-latitudes. Fresh water accumulates in the Northeast Atlantic from where a fresh intermediate water eventually reaches the western boundary. This re-establishes the deep southward pathway of fresh water from the northern North Atlantic. The time scale of this adjustment and of the storage of fresh water in the subpolar Atlantic depends on the exact location of the intermediate water formation in the northern North Atlantic.

One objective of this paper is to test the ocean components of IPCC class coupled climate models, specifically what kind of surface boundary condition would be best suited to reproduce the most important feedbacks of the coupled system. Based on results of several experiments with different surface boundary conditions, a range for the strength of the response can be estimated. Unfortunately, this range is large and there is no easy way to ensure that the response resembles that found in coupled climate models, short of running suites of coupled models. While changes in wind stress and the atmospheric water transports will probably change the results obtained with a simple atmospheric component, results from partially coupled climate models (Dixon et al., 1999; Mikolajewicz and Voss, 2000) indicate that at least the effect of changed wind stresses might be of minor importance compared to that of the surface heat and fresh water flux changes.

From previous results (Stouffer et al., in press) and for theoretical reason we believe that the response of the coupled OGCM—AEBM comes closest to the behaviour of a coupled AOGCM. Here, the counteracting heat and salt advection feedbacks are present and allow a realistic sensitivity of the large scale oceanic circulation to surface perturbations. This configuration also allows a reaction of the sea ice component to these changes. The role of sea ice is potentially important as it affects the ocean—atmosphere heat exchange and especially the radiative balance of the atmosphere (Lohmann and Gerdes, 1998; Winton, 2003). Mixed boundary conditions lead to a somewhat higher sensitivity and exhibit large oscillations of the meridional overturning circulation in the control run. The higher sensitivity was expected from earlier results (Zhang et al., 1993). The mechanism that produces the enhanced sensitivity under mixed boundary conditions is well understood (e.g. Rahmstorf and Willebrand, 1995; Lohmann et al., 1996) and also works in cases of weak restoring of surface salinity combined with fixed atmospheric temperatures. The lack of response in sea ice (Fig. 14) make the response under mixed boundary conditions further unrealistic. Restoring surface salinity, on the other hand, effectively suppresses the salt advection feedback and does not allow the global scale reaction in circulation and hydrographic fields. This is not changed when the perturbation part of the salt anomaly is free to develop (as in the SPLIT experiment) because the changes in salinity induced by circulation anomalies are the far more important part of the response in a more realistic system.

The sensitivity to the form of the surface boundary conditions poses a serious problem for ocean-only and ocean–sea ice experiments. The dependence of OGCM sensitivity on the surface boundary conditions is a general problem as it affects all ocean variability experiments to some degree. Ocean modellers need to find a solution to this problem when future variability experiments (e.g., hindcasts) should be acceptable to the climate community.

The large range of responses to identical surface fresh water flux anomalies documented here calls for the development of simple atmospheric components to be used in ocean–sea ice experiments with variable or anomalous forcing in order to address the following two tasks: (1) to reproduce most aspects of the sensitivity in coupled models without sacrificing the ability to prescribe wind stress, (2) to identify reasons for the different sensitivity of the large scale oceanic circulation in different models. The first task is a precondition for the second. It is not presently achieved and it is in general only partially achievable. Nevertheless, it is important to make progress in this direction as many forced ocean simulations do not provide robust results when certain feedbacks are not adequately considered.

Acknowledgements

We acknowledge the support of the German ministry for research and technology under the DEKLIM program (contract 01 LD 0047). This work was initiated during a visit of RG at the Geophysical Fluid Dynamics Laboratory, Princeton. RG thanks GFDL for the hospitality and financial support. We thank R. Stouffer for fruitful discussions and information about the CMIP water hosing experiments. R. Stouffer and M. Winton made valuable suggestions to improve the manuscript.

References

Beckmann, A., Döscher, R., 1997. A method for improved representation of dense water spreading over topography in geopotential-coordinate models. J. Phys. Oceanogr. 27, 581–591.

Bönisch, G., Schlosser, P., 1995. Deep water formation and exchanges rates in the Greenland/Norwegian seas and the Eurasian Basin of the Arctic Ocean derived from tracer balances. Prog. Oceanogr. 35, 29–52.

Bryan, K., Lewis, L.J., 1979. A water mass model of the world ocean. J. Geophys. Res. 84, 2503–2517.

Cessi, P., Bryan, K., Zhang, R., 2004. Global seiching of thermocline waters between the Atlantic and the Indian–Pacific Ocean Basins. Geophys. Res. Lett. 31, L04302. doi:10.1029/2003GL019091.

Cubasch, U. et al., 2001. Projections of future climate change. In: Houghton, J.T., Ding, Y., Griggs, D.J., Noguer, M., van der Linden, P.J., Xiaosu, D. (Eds.), Climate Change 2001, The Scientific Basis. Cambridge University Press, pp. 525–582.

Cunnigham, S.A., Alderson, S.G., King, B.A., Brandon, M.A., 2003. Transport and variability of the Antarctic Circumpolar Current in Drake Passage. J. Geophys. Res. 108. doi:10.1029/2001JC00114.

Dixon, K.W., Delworth, T.L., Spelman, M.J., Stouffer, R.J., 1999. The influence of transient surface fluxes on North Atlantic overturning in a coupled GCM climate change experiment. Geophys. Res. Lett. 26, 2749–2752.

Gerdes, R., Hurka, J., Karcher, M., Kauker, F., Köberle, C., 2005. Simulated history of convection in the Greenland and Labrador Seas 1948–2001. In: Drange, H. et al. (Eds.), The Nordic Seas, An Integrated Perspective, Geophysical Monograph Series, 158, AGU, Washington, DC, pp. 221–238.

GFDL Global Atmospheric Model Development Team, 2004. The new GFDL global atmosphere and land model AM2-LM2: Evaluation with prescribed SST simulations. J. Climate 17 (24), 4641–4673.

Gnanadesikan, A. et al., in press. GFDL's CM2 global coupled climate models—Part 2: The baseline ocean simulation, J. Climate.

Gordon, A.L., Susanto, R.D., Vranes, K., 2003. Cool Indonesian throughflow as a consequence of restricted surface layer flow. Nature 425, 824–828.

Griffies, S.M., 1998. The Gent-McWilliams skew flux. J. Phys. Oceanogr. 28, 831–841.

Griffies, S.M., 2004. Fundamentals of Ocean Climate Models. Princeton University Press, Princeton, USA, 496 pp.

Griffies, S.M., Hallberg, R.W., 2000. Biharmonic friction with a Smagorinsky viscosity for use in large-scale eddy permitting ocean models. Mon. Weather Rev. 128, 2935–2946.

Griffies, S.M., Gnanadesikan, A., Pacanowski, R.C., Larichev, V.D., Dukowicz, J.K., Smith, R.D., 1998. Isoneutral diffusion in a *z*-coordinate ocean model. J. Phys. Oceanogr. 28, 805–830.

Griffies, S.M., Pacanowski, R.C., Schmidt, R.M., Balaji, V., 2001. Tracer conservation with an explicit free surface method for *z*-coordinate ocean models. Mon. Weather Rev. 129, 1081–1098.

Griffies, S.M., Harrison M.J., Pacanowski R.C., Rosati A., 2004. A Technical Guide to MOM4. GFDL Ocean Group Technical Report No. 5, 337 pp.

Griffies, S.M., Gnanadesikan, A., Dixon, K.W., Dunne, J.P., Gerdes, R., Harrison, M.J., Rosati, A., Russell, J., Samuels, B.L., Spelman, M.J., Winton, M., Zhang, R., 2005. Formulation of an ocean model for global climate simulations. Ocean Sci. 1, 45–79.

Hansen, B., Østerhus, S., 2000. North Atlantic–Nordic Seas exchanges. Prog. Oceanogr. 45, 109–208.

Holloway, G., Sou, T., 2002. Has Arctic Sea ice rapidly thinned? J. Climate 15, 1691–1701.

Hundsdorfer, W., Trompert, R., 1994. Method of lines and direct discretization: a comparison for linear advection. Appl. Numer. Math., 469–490.

Huybrechts, P., de Wolde, J., 1999. The dynamic response of the Greenland and Antarctic ice sheets to multiple-century climate warming. J. Climate 12, 2169–2188.

Jakobssen, M., Chervis, N., Woodward, J., Macnab, R., Coakley, B., 2000. New grid of Arctic bathymetry aids scientists and mapmakers. EOS Trans. Am. Geophys. Union, 81, 89, 93, 96.

Köberle, C., Gerdes, R., 2003. Mechanisms determining the variability of arctic sea ice conditions and export. J. Climate 16, 2843–2858.

Large, W.G., McWilliams, J.C., Doney, S.C., 1994. Oceanic vertical mixing: a review and a model with a vertical *K*-profile boundary layer parameterization. Rev. Geophys. 32, 363–403.

Large, W.G., Danabasoglu, G., Doney, S.C., McWilliams, J.C., 1997. Sensitivity to surface forcing and boundary layer mixing in a global ocean model: annual mean climatology. J. Phys. Oceanogr. 27, 2418–2447.

Large, W.G., Danabasoglu, G., McWilliams, J.C., Gent, P.R., Bryan, F.O., 2001. Equatorial circulation of a global ocean climate model with anisotropic horizontal viscosity. JPO 31, 518–536.

Leaman, K.D., Molinari, R.L., Vertes, P.S., 1987. Structure and variability of the Florida Current at 27N: April 1982–July 1984. J. Phys. Oceanogr. 17, 565–583.

Lee, H.-C., Rosati, A., Spelman, M.J., 2006. Barotropic tidal mixing effects in a coupled climate model: Oceanic conditions on the Northern Atlantic. Ocean Modell. 11, 464–477.

Lohmann, G., Gerdes, R., 1998. Sea ice effects on the sensitivity of the thermohaline circulation. J. Climate 11, 2789–2803.

Lohmann, G., Gerdes, R., Chen, D., 1996. Sensitivity of the thermohaline circulation in coupled oceanic GCM—atmospheric EBM experiments. Climate Dynam. 12, 403–416.

Manabe, S., Stouffer, R.J., 2000. Study of abrupt climate change by a coupled ocean-atmosphere model. Quatern. Sci. Rev. 19, 285–299.

Marshall, J., Schott, F., 1999. Open-ocean convection: observations, theory, and models. Rev. Geophys. 37, 1–64.

Mikolajewicz, U., Voss, R., 2000. The role of the individual air-sea flux components in CO_2-induced changes of the ocean's circulation and climate. Climate Dynam. 16, 627–642.

Murray, R.J., 1996. Explicit generation of orthogonal grids for ocean models. J. Comput. Phys. 126, 251–273.

NOAA, 1988. Data Announcement 88-MGG-02, Digital relief of the surface of the earth. Tech. Rep., NOAA, National Geophysical Data Center, Boulder, Colorado.

Pacanowski, R.C., Gnanadesikan, A., 1998. Transient response in a *z*-level ocean model that resolves topography with partial cells. Mon. Weather Rev. 126, 3248–3270.

Peterson, B.J., Holmes, R.M., McClelland, J.W., Vörösmarty, C.J., Lammers, R.B., Shiklomanov, A.I., Shilomanov, I.A., Rahmstorf, S., 2002. Increasing river discharge to the Arctic Ocean. Science 298, 2171–2173.

Rahmstorf, S., Willebrand, J., 1995. The role of the temperature feedback in stabilizing the thermohaline circulation. J. Phys. Oceanogr. 25, 787–805.

Rahmstorf, S., Marotzke, J., Willebrand, J., 1996. Stability of the thermohaline circulation. In: Krauss, W. (Ed.), The Warmwatersphere of the North Atlantic. Borntraeger, Berlin, pp. 129–157.

Roach, A.T., Aagaard, K., Pease, C.H., Salo, S.A., Weingartner, T., Pavlov, V., Kulakow, M., 1995. On the intermediate depth waters of the Arctic Ocean. In: Johannessen, O.M., Muench, R.D., Overland, J.E. (Eds.), The Polar Oceans and their Role in Shaping the Global Environment, Geophysical Monograph, vol. 85. American Geophysical Union, Washington, DC, pp. 33–46.

Röske, F., 2001. An atlas of surface fluxes based on the ECMWF reanalysis—a climatological database to force global ocean general circulation models. Report 323, Max-Planck-Institut für Meteorologie, Hamburg, Germany, 31 pp.

Röske, F., 2006. A global heat and fresh water forcing dataset for ocean models. Ocean Modell. 11, 235–297.

Rothrock, D.A., Yu, Y., Maykut, G.A., 1999. Thinning of the Arctic sea-ice cover. Geophys. Res. Lett. 26, 3469–3472.

Russell, J.L., Zhang, R., Hurlin, W., 2005. An EBM for GFDL's Flexible Modeling System, GFDL Ocean Group Technical Report, Princeton, 20 pp.

Smagorinsky, J., 1963. General circulation experiments with the primitive equations: I. The basic experiment. Mon. Weather Rev. 91, 99–164.

Smith, R.D., McWilliams, J.C., 2003. Anisotropic horizonal viscosity for ocean models. Ocean Modell. 5, 129–156.

Smith, W.H.F., Sandwell, D.T., 1997. Global seafloor topography from satellite altimetry and ship depth soundings. Science 277, 1957–1962.

Steele, M., Morfley, R., Ermold, W., 2001. PHC: A global ocean hydrography with a high-quality Arctic Ocean. J. Climate 14, 2079–2087.

Stouffer, R.J., Yin, J., Gregory, J.M., Dixon, K.W. Spelman, M.J., Hurlin, W., Weaver, A.J., Eby, M., Flato, G.M., Hasumi, H., Hu, A., Jungclaus, J., Kamenkovich, I.V., Leverman, A., Montoya, M., Murakami, S., Nawrath, S., Oka, A., Peltier, W.R., Robitaille, D.Y., Sokolov, A., Vettoretti, G., Weber, N., in press. Investigating the causes of the response of the thermohaline circulation to past and future climate changes. J.Climate.

Sweby, P., 1984. High-resolution schemes using flux limiters for hyperbolic conservation laws. SIAM J. Numer. Anal. 21, 995–1011.

Sweeney, C., Gnanadesikan, A., Griffies, S.M., Harrison, M.J., Rosati, A.J., Samuels, B.L., 2005. Impacts of shortwave penetration depth on large-scale ocean-circulation and heat transport. J. Phys.Oceanogr. 35, 1103–1119.

Trenberth, K.E., Caron, J., 2001. Estimates of meridional atmosphere and ocean heat transports. J. Climate 14, 3433–3443.

Winton, M., 2000. A reformulated three-layer sea ice model. J. Atmosph. Ocean. Technol. 17, 525–531.

Winton, M., 2003. On the climatic impact of ocean circulation. J. Climate 16, 2875–2889.

Zhang, S., Greatbatch, R.J., Lin, C.A., 1993. A reexamination of the polar halocline catastrophe and implications for coupled ocean-atmosphere modeling. J. Phys. Oceanogr. 23, 287–299.